Geophysical Research Letters

RESEARCH LETTER
10.1029/2023GL107388

Imaging Step Formation in In-Cloud Lightning Initial Development With VHF Interferometry

Yunjiao Pu[1] and **Steven A. Cummer**[1]

[1]Electrical and Computer Engineering Department, Duke University, Durham, NC, USA

Key Points:

- We observed four distinct VHF processes in the development of 300–1,000 m long initial breakdown pulses (IBPs) in in-cloud lightning flashes
- These four processes appear to map to the known processes in a conventional stepped leader, including space stem and space leader formation
- During an initial breakdown step, fast extension over several hundred meters indicates that fast breakdown may be an essential part of in-cloud flash

Supporting Information:

Supporting Information may be found in the online version of this article.

Correspondence to:

S. A. Cummer,
cummer@duke.edu

Citation:

Pu, Y., & Cummer, S. A. (2024). Imaging step formation in in-cloud lightning initial development with VHF interferometry. *Geophysical Research Letters*, *51*, e2023GL107388. https://doi.org/10.1029/2023GL107388

Received 26 NOV 2023
Accepted 15 DEC 2023

Abstract

We investigate sequential processes underlying the initial development of in-cloud lightning flashes in the form of initial breakdown pulses (IBPs) between 7.4 and 9.0 km altitudes, using a 30–250 MHz VHF interferometer. When resolved, IBPs exhibit typical stepped leader features but are notably extensive (>500 m) and infrequent (∼1 millisecond intervals). Particularly, we observed four distinct phases within an IBP stepping cycle: the emergence of VHF sources forming edge structures at previous streamer zone edges (interpreted as space stem/leader development), the fast propagation of VHF along the edge structure (interpreted as the main leader connecting the space leader), the fast extension of VHF beyond the edge structure (interpreted as fast breakdown), and a decaying corona fan. These measurements illustrate clearly the processes involved in the initial development of in-cloud lightning flashes, evidence the conducting main leader forming, and provide insights into other processes known to occur simultaneously, such as terrestrial gamma ray flashes.

Plain Language Summary

The initial development of a lightning flash inside a cloud has long been a mystery. This study utilizes state-of-the-art lightning imaging techniques with a 30–250 MHz VHF interferometer, providing clear images of the processes involved in the initial development of in-cloud lightning flashes. New radio features suggest distinct development phases, including what we interpret as space stems, space leaders, connection between the main leader and the space leader, fast breakdown, and corona fan development within an initial breakdown pulse stepping cycle. This provides evidence of the conducting main leader in the initial breakdown stage. These observations showcase the intricate streamer discharge phenomena during initial lightning development, and shed light on other processes known to occur simultaneously, including Terrestrial Gamma ray Flashes.

1. Introduction

The initial development of a lightning flash inside the cloud has long been, at best, partly understood (Dwyer & Uman, 2014). Not only does the understanding of the underlying streamer and leader physics remain intriguing (e.g., Liu et al., 2022; Lyu, Cummer, Lu, et al., 2016; Petersen et al., 2008), but it also carries significant implications for high-energy radiation, such as terrestrial gamma ray flashes (TGFs), which most commonly occur during this stage of lightning development (e.g., Cummer et al., 2015; Lu et al., 2010; Stanley et al., 2006). Drawing from previous research, the initial development of an in-cloud (IC) lightning flash can be divided into three distinct parts: the initiation stage, characterized by either fast breakdown or non-fast breakdown processes within the first tens of microseconds (Lyu et al., 2019; Rison et al., 2016); the initial breakdown (IB) stage, involving multiple large radio pulses named IB pulses (IBPs) over the first several milliseconds (Marshall et al., 2013; Wu et al., 2015); and the subsequent normal negative stepped leader stage.

Although previous reports show that IBPs exhibit some characteristics reminiscent of a typical stepped leader, radio and optical observations also suggest that the process responsible for IBPs could be predominantly driven by cold streamers and thus physically different from the typical stepped leader with a hot conducting channel (Huang et al., 2022; Stolzenburg et al., 2013). In contrast, recent LOFAR observations (Liu et al., 2022) suggested that IBPs may involve space stem and space leader processes, which are crucial features of typical negative stepped leaders. However, no direct evidence of this has been reported thus far.

Meanwhile, the step formation process involving space stems and space leaders has remained a sustaining mystery in atmospheric electricity as well as in plasma physics and chemistry. Despite numerous reports confirming the existence of space stems/leaders in laboratory long sparks (e.g., Kochkin et al., 2014; Kostinskiy et al., 2018; Les Renardieres Group, 1981; Zhao et al., 2023) and both natural and triggered lightning (e.g., Biagi et al., 2009;

Gamerota et al., 2014; Jiang et al., 2020; Petersen & Beasley, 2013), the detailed evolution of a space stem into a space leader and thus the subsequent leader step has yet to be clarified due to the extremely short time scale of the process (<10 μs near the ground). This poses significant challenges in reliably uncovering the mechanisms underlying space stem and space leader formation (e.g., Babich et al., 2021; Iudin et al., 2018).

In this study, employing state-of-the-art interferometric imaging with a 30–250 MHz VHF interferometer and leveraging the large temporal-spatial scale of IC IB, we unveiled the intricate sequence of step formation processes during IBPs at 7.4–9.0 km altitudes. We found that IBP steps are similar to conventional negative leader steps, but with significantly longer steps (300–1,000 m) and ∼1 millisecond inter-step intervals. New VHF radio features interpreted as the development of space stems (observed as edge structures at the previous corona fan edge) and space leaders (observed as attempted fast propagation of VHF along the edge structure) are identified, providing evidence of the forming conducting main leader. Additionally, we observed fast VHF extension beyond the potential space-leader region where no prior VHF activity was detected, which could be fast breakdown.

2. Instrumentation and Data Processing

The data were collected using a 30–250 MHz broadband VHF interferometer situated near Duke University in Durham, NC, which comprises three discone antennas that form two 52-m-long orthogonal baselines (Pu & Cummer, 2019). Acquisition was performed using a 4-channel 500 MS/s Spectrum Instrumentation digitizer, providing a wide signal bandwidth of up to 250 MHz.

We utilized a 2-step focused interferometry method (Shao et al., 2020) to enhance the imaging quality. While alternative approaches exist, we have found the following procedures yield good images:

1. VHF signals were filtered within a passband of 30–250 MHz, with broadcast transmitter noise eliminated.
2. Pulse peaks in the denoised waveforms were identified by finding local maxima with a minimum separation of 50 ns.
3. Signal windows centered at each peak were defined, and a 2-step focused cross-correlation was applied to the windowed signals. The window widths were set to 6 and 1 microsecond, respectively.

This approach results in significantly overlapped cross-correlation windows with a sliding size as short as 50 ns. As argued by Shao et al. (2020), for continuously moving sources, even a single data point difference can provide new information about their positions. For static sources, the points cluster near the same location, which is over-determined but not erroneous. Although artifacts could occur due to sudden shifts in discharge location, they can be easily identified by their non-physical high speeds close to or exceeding the speed of light (Shao et al., 2020).

Based on uncertainty simulations (Shao et al., 2021), the current 3-antenna VHF interferometer demonstrates angular uncertainty below 0.1° for 30–250 MHz signals with SNR exceeding 10 dB. To validate with real lightning data, we focused on initial weak emissions immediately following flash initiation, with SNR mostly below 5 dB during 0–1.8 ms (Figure 1c), and found a spatial spread of 0.3°. This represents a reasonable upper bound of uncertainty and aligns with the simulation results. Therefore, the wide spatial extent of the fan-shaped sources in our images (>2° and >10 dB, Figure 1), which we call corona fan, is not due to imaging artifacts but represents genuine lightning characteristics.

3. Results

3.1. Initial 0–10 Milliseconds of an In-Cloud Lightning Flash

Figure 1 shows the initial lightning development within 0–10 milliseconds for a well-resolved IC flash observed by our VHF interferometer on 5 August 2022, at 02:06:29 UTC. To facilitate our description, we have labeled three distinct VHF bursts associated with IB pulses (IBPs) (Belz et al., 2020; Kolmasova et al., 2018). They correspond to separate groups of initially fast propagating sources and subsequently slowly expanding fan-shaped sources, defining three IBP steps (IS1, IS2, and IS3) and their corona fans (CF1, CF2, and CF3) in Figure 1a.

According to the U.S. National Lightning Detection Network (NLDN), the flash horizontal range to the interferometer is 4.5 km for IS2 and 4.4 km for IS3, with peak currents of 9 and 7 kA, respectively. This corresponds to approximate 300 m per 1° elevation and 2° azimuth near 60° elevation, leading to an altitude progression of 7.4–9.0 km for the three IBP steps. The reported NLDN uncertainty for both IBPs is a 200 × 200 m 50% error ellipse, resulting in an angular resolution shift of only ∼10 m per 1° elevation and is thus negligible.

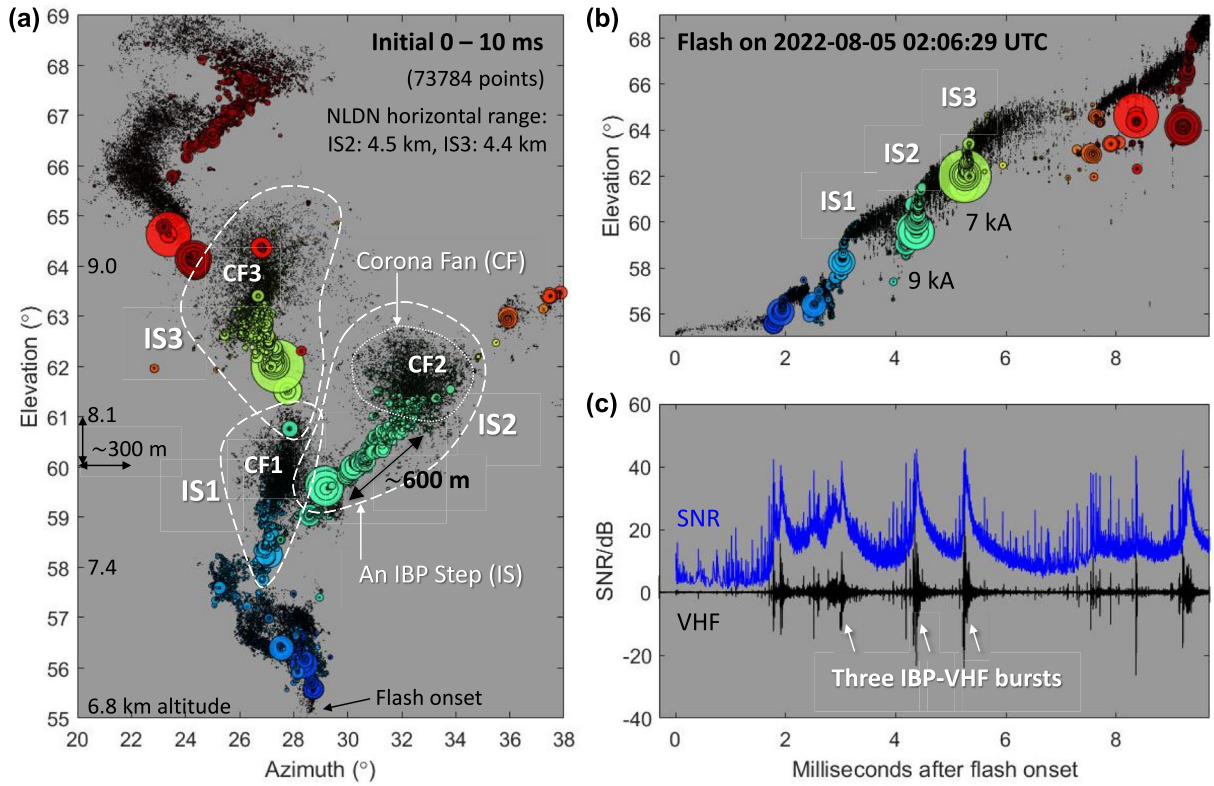

Figure 1. Overview of the initial development of an in-cloud lightning flash in 0–10 milliseconds on 5 August 2022, at 02:06:29 UTC. (a) A 2D map from our interferometer. Source marker size corresponds to the center point power of the 1-μs waveform. Three distinct IBP steps with corona fans are marked with closed loops for further examination. (b) Time-dependent source elevation. (c) Time-dependent VHF waveform and signal-to-noise ratio. IBP: initial breakdown pulse.

The source point size corresponds to the peak/center-point power of each 1-μs window, providing an estimate of instantaneous VHF power. The signal-to-noise ratio (SNR) is computed for each 1-μs windowed waveform, serving as a measure of the received signal quality and an indicator of the angular accuracy in the imaging.

Upon analyzing VHF emissions and imaged sources, we find that strong VHF bursts occur after initial weak emissions in the first 2 ms of detectable VHF activity. These weak VHF sources propagate upward at a velocity of $\sim 1.2 \times 10^5$ m/s over 200 m, preconditioning the subsequent IBP development. In the next section, we focus on the development of three IBP steps.

3.2. Evolution of Three IBP Steps

Figure 2 depicts the evolution of three distinct IBP steps during 3–6.2 ms. The start and end of an IBP step are defined where the SNR of VHF emissions reaches a minimum value (approximately 10 dB above our noise level) during the inter-step interval, marking the end of the previous step and the start of a new one. The precise time windows for these three IBP steps are labeled in Figure 2b, and the process is further divided for detailed examination of both stepping and inter-step intervals.

In Figures 2a.1, 2a.5, and 2a.8, strong VHF bursts and their trailing decaying emissions are observed during the progression of an IBP step, featuring intensive, narrow, and fast-propagating VHF in the initial 50–100 μs, transitioning to weaker, more spatially extensive, and slowly propagating corona fans lasting 500–800 μs at the end.

As the corona fans decrease in VHF intensity and propagation speeds, notable VHF pulses emerge at their edges in Figures 2a.2, 2a.3, and 2a.6, resulting in a modest intensification of VHF emissions. Soon after that, much stronger discrete VHF pulses (~0.2 μs duration) occur at the edges immediately before the advancement of the subsequent step, as illustrated in Figures 2a.4 and 2a.7. These are termed edge structures and will be further analyzed in Section 4.

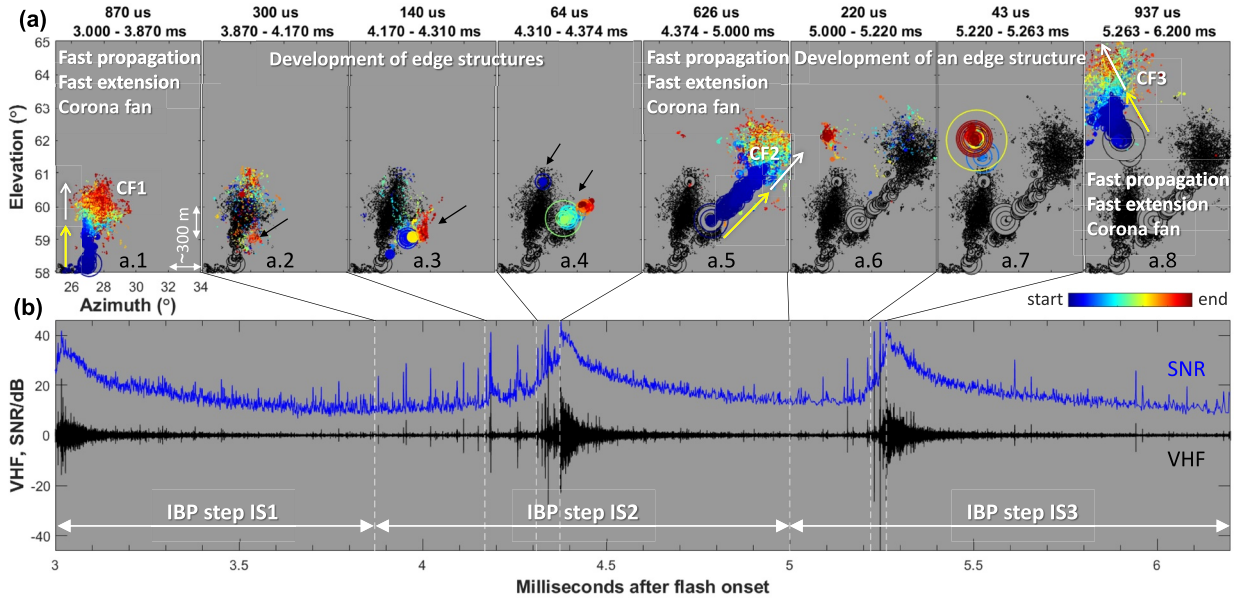

Figure 2. VHF emission sources and waveforms illustrating the evolution of three IBP steps. Individual IBP steps are separated at the minimum signal-to-noise ratio in inter-step intervals. IBP: initial breakdown pulse.

IBP steps IS2 and IS3 initiate sequentially at the CF1 edge, revealing the branching process during IC initial development. According to our observation, the branching is closely related to the multiple edge structures around the same corona fan. Despite IS2 occurring first, the edge structures responsible for the two branches initiate nearly simultaneously, as evident from emissions at the top and lateral sides of CF1 in Figure 2a.4. Reactivation and development of the top edge structure for IS3 are observed in Figure 2a.6, approximately 1 ms after IS2 completes. In the next section, we will study the detailed IBP step formation process using IS2 as an example.

3.3. Distinct Development Phases Comprising an IBP Step

Figure 3 illustrates the four distinct phases that encompass the formation of a complete IBP step for IS2.

Phase 1: *Emergence of VHF Sources Forming an Edge Structure at the Previous Corona Fan Edge* (Figures 3a.1 and 3b.1)—Discrete VHF pulses lasting ~0.2 μs emerge at the edge of the previous decaying corona fan CF1, primarily located on the right side, along with a single source at the top. The localized emissions at the right edge form a structure in the direction outward from the CF1 core over a length of 200 m, but are spatially unorganized within this length without consistent propagation direction. Besides the impulsive signatures, the VHF SNR begins to build up in this phase.

Phase 1b: *Fast propagation of VHF along the Edge Structure* (*first attempt*) (Figures 3a.2 and 3b.2)—Along the newly formed edge structure, outward propagating sources are observed at a fast speed of $\sim 1 \times 10^7$ m/s within 24 μs. The VHF emissions are continuous but not significantly enhanced. This phase appeared in half of the IBPs analyzed (additional IBPs shown in the Supporting Information S1).

Phase 2: *Fast Propagation of VHF along the Edge Structure* (Figures 3a.3 and 3b.3)—The VHF reinitiates at the back end of the edge structure with a strong narrow pulse, and rapidly traverses this preconditioned region at a velocity of $\sim 4.3 \times 10^7$ m/s, comparable to that of a strong dart leader. The VHF emissions in this phase reach the maximum intensity of the entire IBP step.

Phase 3: *Fast Extension of VHF beyond the Edge Structure* (Figures 3a.4 and 3b.4)—The fast VHF in Phase 3 extends beyond the edge structure and immediately penetrates into the air where no previous VHF activities were detected, for approximately 400 m long and 100 m wide, while maintaining a slower but still high speed of $\sim 1 \times 10^7$ m/s. The VHF emissions in this phase slightly decrease but remain at a high SNR above 30 dB.

Phase 4: *Slow VHF Propagation of the Corona Fan* (Figures 3a.5 and 3b.5)—The observed VHF activity continues to decelerate and expand extensively in space, forming a fan-shaped corona reminiscent of those observed

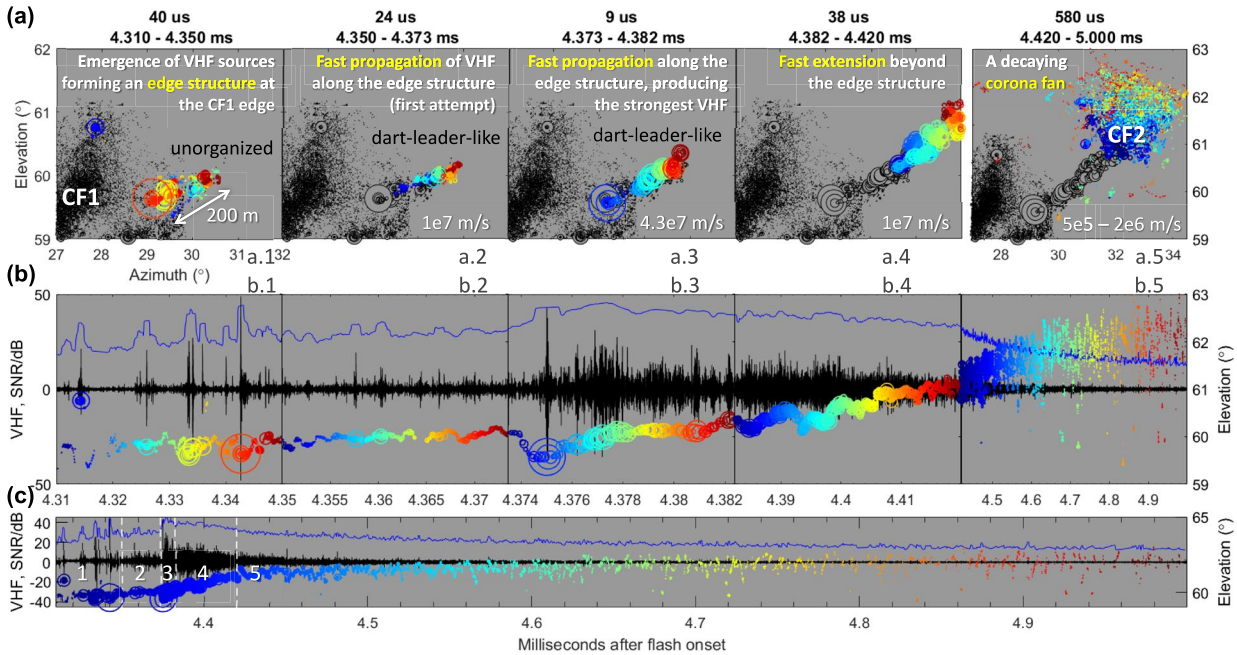

Figure 3. VHF emission source map and waveforms illustrate distinct development phases within an IBP stepping cycle for IS2 marked in Figures 1 and 2. IBP: initial breakdown pulse.

in laboratory experiments (Kostinskiy et al., 2018). The corona fan spans an area of over 500 × 500 m, with the outward propagation speed steadily decreases from 2×10^6 to 5×10^5 m/s over approximately 600 μs. The VHF emissions in this phase decay continuously to ∼10 dB until the next new edge structure manifests for the next IBP step.

Note that these four distinct phases may not always be well resolved due to the distance and the viewing angle, especially Phase 1b. To maintain generalization, we present more examples in Figures S1–S5 in Supporting Information S1, where distinct IBP steps with similar development phases are depicted in VHF, in conjunction with the available low-frequency (LF) magnetic measurements.

4. Analysis

4.1. Interpretation of Dynamics of IBP Step Formation

The three IBP steps observed between 7.4 and 9.0 km altitudes exhibit typical negative leader stepping features but with massive steps (300–1,000 m) occurring less frequently (∼1 millisecond intervals), in contrast to cloud-to-ground negative leader steps that are shorter (∼10 m) and more frequent (5–50 microsecond intervals) (Chen et al., 1999). This scale difference cannot be simply scaled by altitude with similarity laws (Pasko et al., 1998; Scholten et al., 2021) and merits further study.

To understand the observed IBP stepping characteristics in VHF, the key question is: What physical processes produce VHF emissions? Theoretical calculations suggest that VHF emissions result from rapid changes in current moments on a nanosecond timescale (Liu et al., 2019; Qin et al., 2012). To the best of our knowledge, two scenarios have been demonstrated in simulations, including exponentially growing streamers in high electric fields (Liu et al., 2019; Shi et al., 2016) and colliding streamers emitting at VHF and UHF (Luque, 2017; Shi et al., 2019).

In Figure 4a, we introduce an IBP stepping model primarily relying on the streamer-growth theory (Liu et al., 2019) to interpret the data. This theory is the only fully formed theory of VHF generation and aligns with our previous VHF-UHF spectral measurements (Pu et al., 2022). Although accelerating streamers have been explored as a source of VHF emissions, uncertainty remains about the processes generating VHF and higher frequencies, making it an active area of research.

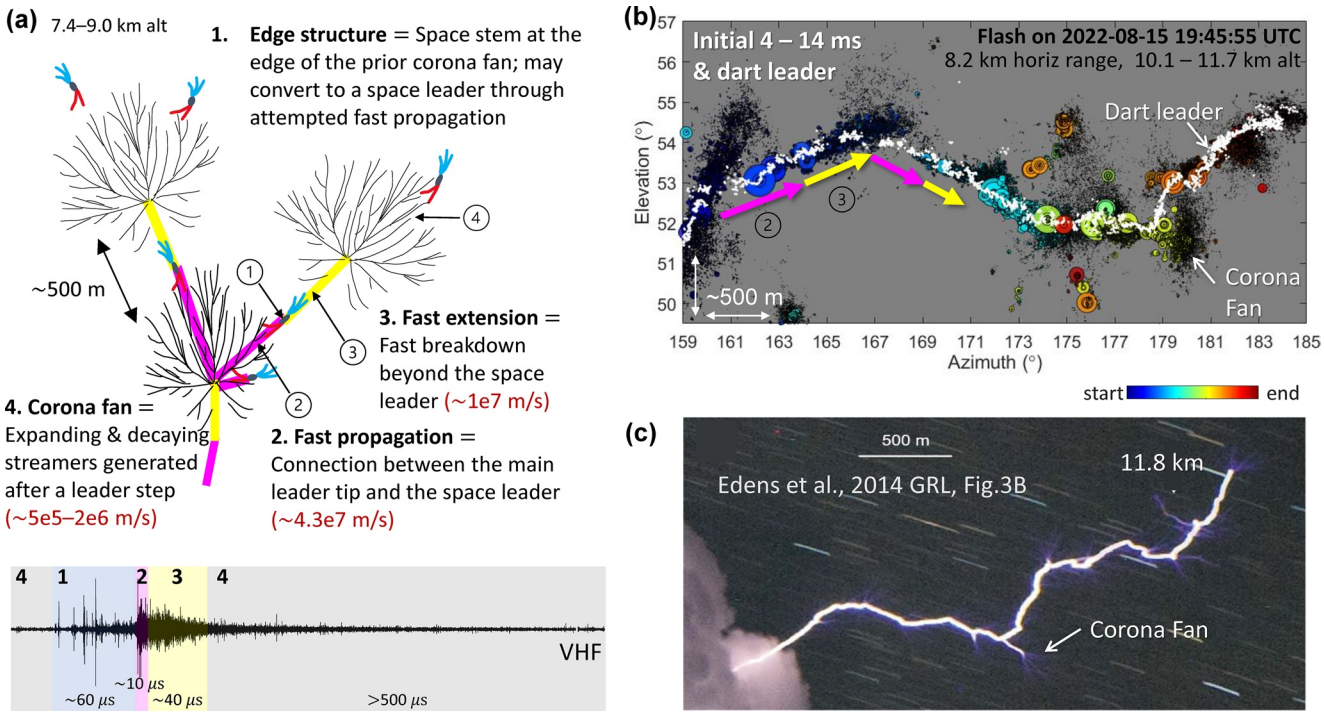

Figure 4. Illustration of initial lightning development based on three IBP steps in Figure 1, and a comparison between a VHF-imaged initial leader and a photography of a cloud-to-air leader. (a) A diagram summarizing the key components in three IBP steps. (b) Imaged initial lightning development on 15 August 2022, at 19:45:55 UTC, with a dart leader traversing the initial main leader channel. (c) Photograph of a cloud-to-air leader adapted from Edens et al. (2014). IBP: initial breakdown pulse.

4.1.1. Edge Structures, Space Stems, and Space Leaders

We suspect that the edge structures we observed at the corona fan edges are space stems, which are electrode-like plasma structures ahead of a conducting leader tip (Les Renardieres Group, 1981). In our observations, discrete strong VHF pulses scatter along a 100–200 m long linear structure for over 50 μs at the previous corona fan edge before the subsequent IBP step. These timing and location characteristics suggest that they are VHF signatures of a forming space stem. Similar structures ahead of the negative leader tip were observed optically in laboratory experiments and triggering lightning, which were interpreted as space stems but with significantly shorter length (a few millimeters to meters near the ground) (Biagi et al., 2009; Zhao et al., 2023). In addition, multiple edge structures, or space stems, appear at the sides of the preceding corona fan and evolve into separate steps, offering a natural explanation for the branching and zigzagging nature seen in negative stepped leaders (e.g., Jiang et al., 2017; Qi et al., 2016).

The VHF emissions forming edge structures could be generated by new exponentially growing streamers of the space stem, or collisions between positive streamers of the space stem and negative streamers of the main leader tip. These speculations may be validated in future work by detecting UHF emissions from colliding streamers, as predicted by simulations (Luque, 2017; Shi et al., 2019).

Regarding the space leader, we suspect that the first attempted fast propagation of VHF along the newly formed edge structure, or the space stem, enhances conductivity and converts the perhaps poorly conducting space stem into a conducting space leader. This process, reminiscent of a dart leader, might be triggered by the high electric potential difference at the inner positive end of the space stem. However, we acknowledge that the attempted fast propagation may not always occur, and alternative discharge forms may exist to transform a space stem into a space leader.

4.1.2. Fast Propagation of VHF Connecting the Main Leader and the Space Leader

We suggest that there is a connection between the invisible main leader tip and the space leader which formed a leader section (labeled as number two in Figure 4a). The observed strongest dart-leader-like VHF (~4.3×10^7 m/s)

is likely driven by the strong electric potential between the main leader tip and the space leader, suggesting the presence of a conducting main leader and a connection between the two parts. However, the precise location of the main leader tip remains unclear based on available imaging. Additional evidence demonstrating this connection is discussed in Section 4.2.

It is worth noting that our observation shows negative dart-leader-like VHF propagating outward from the positive end of the space leader, deviating from previous depictions of streamers emerging from both ends (e.g., Bazelyan & Raizer, 2000; Petersen et al., 2008). While a bidirectional connection is possible, with positive streamers moving backward to the main leader, the weak positive breakdown may go undetected in VHF when the forward negative breakdown predominates.

4.1.3. Fast Extension Beyond the Space Leader Could Be Fast Breakdown

In our observations, the fast VHF extends beyond the space leader, penetrating into perhaps undisturbed air with no prior VHF activity. It fills a region over 400 m long and 100 m wide with strong VHF power while maintaining a rapid speed of $\sim 1 \times 10^7$ m/s, typical of fast breakdown in NBEs (Rison et al., 2016; Tilles et al., 2019).

It is important to highlight that this fast breakdown process was recently observed in cloud-to-ground IBPs simultaneous with downward TGFs recorded by the Telescope Array Surface Detector (Belz et al., 2020) and in a 247-kA energetic in-cloud-pulse (EIP) (Tilles et al., 2020) tightly connected to upward TGFs (Lyu, Cummer, Briggs, et al., 2016). Therefore, the fast extension phase observed in this study within the IC IBP step could be closely related to TGF generation. The presence of this process spanning hundreds of meters in only tens of microseconds indicates a large-scale high electric field, which is essential for the relativistic runaway electron avalanche process leading to TGFs. With our IBP having an NLDN-reported peak current of only 9 kA, further investigation into how the peak current affects IBP stepping characteristics and TGF generation is interesting. A machine learning study on identifying lower-peak-current EIPs was conducted by Pu et al. (2023) in this direction.

We anticipate that part of the fast breakdown streamers could transition to a conducting leader section, as labeled with number three in Figure 4a. The transformation could be facilitated by the heating through subsequent corona fan development in the 500–800 μs interstep interval, and should be completed to serve as the new main leader tip before the next step. However, the length of the fast breakdown section that will convert to a conducting leader is unknown, and Figure 4b shows additional observations on this point.

4.1.4. The Decaying Corona Fan Challenges the Physical Interpretation of VHF Emissions

VHF emissions continuously decrease after the fast extension phase, forming a corona fan with extensively expanding streamers and decreasing speeds. This stage represents the IBP development during the inter-step intervals, constituting the majority (>80%, 500–800 μs) of the IBP stepping cycle. As VHF intensity diminishes, new space stems emerge at the corona fan edge, initiating a new stepping cycle.

However, it's important to note that decaying and branching streamers are generally not considered VHF emitters upon exiting high electric field regions (Shi et al., 2019). One plausible interpretation might be that the branching streamer tree can be seen as an ensemble of individual streamers starting randomly and fluctuating on a nanosecond timescale, collectively producing VHF emissions (Liu et al., 2019, 2020).

4.2. Relationship Between the Main Leader and Corona Fans

To clarify the main leader location, which was unclear in VHF maps in Figures 1–3, we investigate an additional IC flash from 15 August 2022, at 19:45:55 UTC, in Figure 4b. This flash, farther from our interferometer than the previous one, has less well-resolved IBP stepping features but contains a subsequent dart leader (white dots) traversing IB regions. Meanwhile, Figure 4c compares this with a photo of a cloud-to-air leader near 11.8 km altitude (Edens et al., 2014).

It is noteworthy that many features in both VHF and optical images are consistent and interpretable:

1. VHF dart leader path aligns with the luminous main leader channel in the photo.
2. VHF corona fans match purple filamentary streamers in the photo.
3. Edge structures (space stems) at lateral sides occur consistently in both, causing alternating steps and zigzagging channels.

4. Two labeled corona fans show wide extension and significant direction change during steps. The bright leader section (∼100 m) in the photo suggests transformation into a hot conducting channel, possibly heated by corona fan development.

Moreover, the initially invisible VHF connecting leader becomes distinguishable due to the dart leader (No. 2, pink arrows). Additionally, part of VHF fast breakdown streamers transforms into the conducting main leader channel (No. 3, yellow arrows).

5. Summary

This study unveils clearly the processes involved in the initial development of in-cloud lightning flashes with 30–250 MHz VHF interferometry. The IB pulses (IBPs) exhibit stepping characteristics similar to typical negative stepped leaders but with notably longer steps and inter-step intervals. New VHF radio features show distinct sequential development phases within an IBP stepping cycle (Section 3), which we interpret as space stems, space leaders, connection between the main leader and the space leader, fast breakdown, and corona fan development, providing evidence of the conducting main leader in the IB stage. Questions on the physical connection between streamer processes and VHF emissions are discussed in Section 4 and warrant further exploration. Moreover, these measurements provide insights into other processes known to occur simultaneously, including TGFs.

Data Availability Statement

This work complies with the AGU data policy. The data analyzed in the study are available on the data repository website at http://doi.org/10.5281/zenodo.8371237 (Pu & Cummer, 2023).

Acknowledgments
This study is supported by the National Science Foundation Dynamic and Physical Meteorology program through Grant AGS-2026304. The authors thank Fanchao Lyu for his contribution to the VHF system construction. We thank Brian Hare for providing constructive suggestions on the manuscript and Ningyu Liu for helpful discussions on streamer physics.

References

Babich, L., Kutsyk, I., Bochkov, E., Köhn, C., & Neubert, T. (2021). General processes responsible for the space leader birth in streamer coronas of negative leaders. *Plasma Research Express*, *3*(4), 045003. https://doi.org/10.1088/2516-1067/ac3018

Bazelyan, E. M., & Raizer, Y. P. (2000). Lightning physics and lightning protection.

Belz, J. W., Krehbiel, P. R., Remington, J., Stanley, M. A., Abbasi, R. U., LeVon, R., et al. (2020). Observations of the origin of downward terrestrial gamma-ray flashes. *Journal of Geophysical Research: Atmospheres*, *125*(23). https://doi.org/10.1029/2019jd031940

Biagi, C. J., Jordan, D. M., Uman, M. A., Hill, J. D., Beasley, W. H., & Howard, J. (2009). High-speed video observations of rocket-and-wire initiated lightning. *Geophysical Research Letters*, *36*(15), 5. https://doi.org/10.1029/2009gl038525

Chen, M. L., Takagi, N., Watanabe, T., Wang, D. H., Kawasaki, Z. I., & Liu, X. S. (1999). Spatial and temporal properties of optical radiation produced by stepped leaders. *Journal of Geophysical Research*, *104*(D22), 27573–27584. https://doi.org/10.1029/1999jd900846

Cummer, S. A., Lyu, F., Briggs, M. S., Fitzpatrick, G., Roberts, O. J., & Dwyer, J. R. (2015). Lightning leader altitude progression in terrestrial gamma-ray flashes. *Geophysical Research Letters*, *42*(18), 7792–7798. https://doi.org/10.1002/2015gl065228

Dwyer, J. R., & Uman, M. A. (2014). The physics of lightning. *Physics Reports-Review Section of Physics Letters*, *534*(4), 147–241. https://doi.org/10.1016/j.physrep.2013.09.004

Edens, H. E., Eack, K. B., Rison, W., & Hunyady, S. J. (2014). Photographic observations of streamers and steps in a cloud-to-air negative leader. *Geophysical Research Letters*, *41*(4), 1336–1342. https://doi.org/10.1002/2013gl059180

Gamerota, W. R., Idone, V. P., Uman, M. A., Ngin, T., Pilkey, J. T., & Jordan, D. M. (2014). Dart-stepped- leader step formation in triggered lightning. *Geophysical Research Letters*, *41*(6), 2204–2211. https://doi.org/10.1002/2014gl059627

Huang, A., Cummer, S. A., Pu, Y., Chanrion, O. A., Neubert, T., Reglero, V., & Østgaard, N. (2022). Transition in optical and radio features during the early development of negative intracloud leader. *Geophysical Research Letters*, *49*(22), e2022GL100594. https://doi.org/10.1029/2022gl100594

Iudin, D., Syssoev, A., & Popov, N. (2018). Generation of stems in streamer corona of negative leader. In *Paper presented at proceedings of XVI international conference on atmospheric electricity*.

Jiang, R. B., Qie, X., Li, Z. X., Zhang, H., Li, X., Yuan, S., et al. (2020). Luminous crown residual vs. bright space segment: Characteristical structures for the intermittent positive and negative leaders of triggered lightning. *Geophysical Research Letters*, *47*(21), e2020GL088107. https://doi.org/10.1029/2020gl088107

Jiang, R. B., Qie, X. S., Zhang, H. B., Liu, M. Y., Sun, Z. L., Lu, G. P., et al. (2017). Channel branching and zigzagging in negative cloud-to-ground lightning. *Scientific Reports*, *7*(1), 3457. https://doi.org/10.1038/s41598-017-03686-w

Kochkin, P. O., van Deursen, A. P., & Ebert, U. (2014). Experimental study of the spatio-temporal development of metre-scale negative discharge in air. *Journal of Physics D: Applied Physics*, *47*(14), 145203. https://doi.org/10.1088/0022-3727/47/14/145203

Kolmasova, I., Santolík, O., Defer, E., Rison, W., Coquillat, S., Pedeboy, S., et al. (2018). Lightning initiation: Strong pulses of VHF radiation accompany preliminary breakdown. *Scientific Reports*, *8*(1), 3650. https://doi.org/10.1038/s41598-018-21972-z

Kostinskiy, A. Y., Syssoev, V. S., Bogatov, N. A., Mareev, E. A., Andreev, M. G., Bulatov, M. U., et al. (2018). Abrupt elongation (stepping) of negative and positive leaders culminating in an intense corona streamer burst: Observations in long sparks and implications for lightning. *Journal of Geophysical Research: Atmospheres*, *123*(10), 5360–5375. https://doi.org/10.1029/2017jd027997

Les Renardieres Group. (1981). Negative discharges in long air gaps at Les Renardieres-1978 results and conclusions, Electra (Vol. *74*).

Liu, N. Y., Dwyer, J. R., & Tilles, J. N. (2020). Electromagnetic radiation spectrum of a composite system. *Physical Review Letters*, *125*(2), 6. https://doi.org/10.1103/PhysRevLett.125.025101

Liu, N. Y., Dwyer, J. R., Tilles, J. N., Stanley, M. A., Krehbiel, P. R., Rison, W., et al. (2019). Understanding the radio Spectrum of thunderstorm narrow bipolar events. *Journal of Geophysical Research: Atmospheres*, *124*(17–18), 10134–10153. https://doi.org/10.1029/2019jd030439

Liu, N. Y., Scholten, O., Hare, B. M., Dwyer, J. R., Sterpka, C. F., Kolmašová, I., & Santolík, O. (2022). LOFAR observations of lightning initial breakdown pulses. *Geophysical Research Letters*, *49*(6), e2022GL098073. https://doi.org/10.1029/2022gl098073

Lu, G. P., Blakeslee, R. J., Li, J. B., Smith, D. M., Shao, X. M., McCaul, E. W., et al. (2010). Lightning mapping observation of a terrestrial gamma-ray flash. *Geophysical Research Letters*, *37*(11), 5. https://doi.org/10.1029/2010gl043494

Luque, A. (2017). Radio frequency electromagnetic radiation from streamer collisions. *Journal of Geophysical Research: Atmospheres*, *122*(19), 10497–10509. https://doi.org/10.1002/2017JD027157

Lyu, F. C., Cummer, S. A., Briggs, M., Marisaldi, M., Blakeslee, R. J., Bruning, E., et al. (2016). Ground detection of terrestrial gamma ray flashes from distant radio signals. *Geophysical Research Letters*, *43*(16), 8728–8734. https://doi.org/10.1002/2016gl070154

Lyu, F. C., Cummer, S. A., Lu, G. P., Zhou, X., & Weinert, J. (2016). Imaging lightning intracloud initial stepped leaders by low-frequency interferometric lightning mapping array. *Geophysical Research Letters*, *43*(10), 5516–5523. https://doi.org/10.1002/2016gl069267

Lyu, F. C., Cummer, S. A., Qin, Z. L., & Chen, M. L. (2019). Lightning initiation processes imaged with very high frequency broadband interferometry. *Journal of Geophysical Research: Atmospheres*, *124*(6), 2994–3004. https://doi.org/10.1029/2018jd029817

Marshall, T., Stolzenburg, M., Karunarathne, S., Cummer, S., Lu, G. P., Betz, H. D., et al. (2013). Initial breakdown pulses in intracloud lightning flashes and their relation to terrestrial gamma ray flashes. *Journal of Geophysical Research: Atmospheres*, *118*(19), 10907–10925. https://doi.org/10.1002/jgrd.50866

Pasko, V. P., Inan, U. S., & Bell, T. F. (1998). Spatial structure of sprites. *Geophysical Research Letters*, *25*(12), 2123–2126. https://doi.org/10.1029/98gl01242

Petersen, D. A., & Beasley, W. H. (2013). High-speed video observations of a natural negative stepped leader and subsequent dart-stepped leader. *Journal of Geophysical Research: Atmospheres*, *118*(21), 12110–12119. https://doi.org/10.1002/2013jd019910

Petersen, D. A., Bailey, M., Beasley, W. H., & Hallett, J. (2008). A brief review of the problem of lightning initiation and a hypothesis of initial lightning leader formation. *Journal of Geophysical Research*, *113*(D17), D17205. https://doi.org/10.1029/2007jd009036

Pu, Y. J., & Cummer, S. A. (2019). Needles and lightning leader dynamics imaged with 100–200 MHz broadband VHF interferometry. *Geophysical Research Letters*, *46*(22), 13556–13563. https://doi.org/10.1029/2019gl085635

Pu, Y. J., & Cummer, S. (2023). Imaging step formation in in-cloud lightning initial development with VHF interferometry [Dataset]. Zenodo. https://doi.org/10.5281/zenodo.8371237

Pu, Y. J., Cummer, S. A., Lyu, F., Zheng, Y., Briggs, M. S., Lesage, S., et al. (2023). Unsupervised clustering and supervised machine learning for lightning classification: Application to identifying EIPs for ground-based TGF detection. *Journal of Geophysical Research: Atmospheres*, *128*(9), e2022JD038369. https://doi.org/10.1029/2022jd038369

Pu, Y. J., Liu, N. Y., & Cummer, S. A. (2022). Quantification of electric fields in fast breakdown during lightning initiation from VHF-UHF power spectra. *Geophysical Research Letters*, *49*(5), e2021GL097374. https://doi.org/10.1029/2021GL097374

Qi, Q., Lu, W. T., Ma, Y., Chen, L. W., Zhang, Y. J., & Rakov, V. A. (2016). High-speed video observations of the fine structure of a natural negative stepped leader at close distance. *Atmospheric Research*, *178*, 260–267. https://doi.org/10.1016/j.atmosres.2016.03.027

Qin, J. Q., Celestin, S., & Pasko, V. P. (2012). Low frequency electromagnetic radiation from sprite streamers. *Geophysical Research Letters*, *39*(22), 5. https://doi.org/10.1029/2012gl053991

Rison, W., Krehbiel, P. R., Stock, M. G., Edens, H. E., Shao, X. M., Thomas, R. J., et al. (2016). Observations of narrow bipolar events reveal how lightning is initiated in thunderstorms. *Nature Communications*, *7*(1), 12. https://doi.org/10.1038/ncomms10721

Scholten, O., Hare, B., Dwyer, J., Liu, N., Sterpka, C., Buitink, S., et al. (2021). Distinguishing features of high altitude negative leaders as observed with LOFAR. *Atmospheric Research*, *260*, 105688. https://doi.org/10.1016/j.atmosres.2021.105688

Shao, X.-M., Ho, C., Bowers, G., Blaine, W., & Dingus, B. (2020). Lightning interferometry uncertainty, beam steering interferometry, and evidence of lightning being ignited by a cosmic ray shower. *Journal of Geophysical Research: Atmospheres*, *125*(19), e2019JD032273. https://doi.org/10.1029/2019jd032273

Shao, X.-M., Ho, C., Meierbachtol, C. S., & Anderson, D. (2021). Lightning interferometric processing and uncertainty analysis for general noncoplanar antenna arrays. *Earth and Space Science Open Archive*, *16*.

Shi, F., Liu, N. Y., Dwyer, J. R., & Ihaddadene, K. M. A. (2019). VHF and UHF electromagnetic radiation produced by streamers in lightning. *Geophysical Research Letters*, *46*(1), 443–451. https://doi.org/10.1029/2018gl080309

Shi, F., Liu, N. Y., & Rassoul, H. K. (2016). Properties of relatively long streamers initiated from an isolated hydrometeor. *Journal of Geophysical Research: Atmospheres*, *121*(12), 7284–7295. https://doi.org/10.1002/2015jd024580

Stanley, M. A., Shao, X. M., Smith, D. M., Lopez, L. I., Pongratz, M. B., Harlin, J. D., et al. (2006). A link between terrestrial gamma-ray flashes and intracloud lightning discharges. *Geophysical Research Letters*, *33*(6), L06803. https://doi.org/10.1029/2005gl025537

Stolzenburg, M., Marshall, T. C., Karunarathne, S., Karunarathna, N., Vickers, L. E., Warner, T. A., et al. (2013). Luminosity of initial breakdown in lightning. *Journal of Geophysical Research: Atmospheres*, *118*(7), 2918–2937. https://doi.org/10.1002/jgrd.50276

Tilles, J. N., Krehbiel, P. R., Stanley, M. A., Rison, W., Liu, N., Lyu, F., et al. (2020). Radio interferometer observations of an energetic in-cloud pulse reveal large currents generated by relativistic discharges. *Journal of Geophysical Research: Atmospheres*, *125*(20), e2020JD032603. https://doi.org/10.1029/2020jd032603

Tilles, J. N., Liu, N. Y., Stanley, M. A., Krehbiel, P. R., Rison, W., Stock, M. G., et al. (2019). Fast negative breakdown in thunderstorms. *Nature Communications*, *10*(1), 1648. https://doi.org/10.1038/s41467-019-09621-z

Wu, T., Yoshida, S., Akiyama, Y., Stock, M., Ushio, T., & Kawasaki, Z. (2015). Preliminary breakdown of intracloud lightning: Initiation altitude, propagation speed, pulse train characteristics, and step length estimation. *Journal of Geophysical Research: Atmospheres*, *120*(18), 9071–9086. https://doi.org/10.1002/2015jd023546

Zhao, X., Popov, N. A., Gan, Q., Ding, Y., Du, Y., & He, J. (2023). On a possible mechanism of space stem formation in negative long sparks. *Geophysical Research Letters*, *50*(12), e2023GL102834. https://doi.org/10.1029/2023gl102834